Scientific
Research

The Effect of Initial Oxidation on Long-Term Oxidation of NiCoCrAlY Alloy

Chao Zhu, Xiaoyu Wu, Yuan Wu, Gongying Liang

MOE Key Laboratory for Nonequilibrium Synthesis and Modulation of Condensed Matter,
School of Science, Xi'an Jiaotong University, Xi'an, China
E-mail: *gyliang@mail.xjtu.edu.cn*

Abstract

The initial oxidation behavior of Ni-6.5Co-17.8Cr-3.7Al-0.5Y alloy is investigated at 800°C-1000°C. X-ray diffraction results show that the dominant Cr_2O_3 phase and secondary α-Al_2O_3 and NiO phases are observed on the surface of samples at all initial stages (oxidized for 16 hours). $YAlO_3$ and θ-Al_2O_3 can only be detected at low temperature (800°C) while the spinel $NiCr_2O_4$ is only observed at 900°C and 1000°C. Though the growth rates of α-Al_2O_3 and Cr_2O_3 are comparable at 900°C, the former becomes much lower than the latter when the temperature changes to 1000°C. Scanning electron microscopy (SEM) images show that the α-Al_2O_3 grows from some irregular ditches in the chromia scale at 900°C. However, cracking and spalling are more serious at 1000°C without α-Al_2O_3-grown-ditches, which is in accordance with the growth rates of these oxides at different temperatures. The cracking can be explained by the results of Raman determination which indicate that the stress on the surface of specimen oxidized at 1000°C is higher than that at 900°C. Owing to this condition, a preoxidation treatment on the NiCoCrAlY alloy for 16 hours is prepared at 900°C, and then thermal cycling oxidation test is conducted at 1000°C for 200 hours. The result indicates that the initial preoxidation treatment at 900°C improves the oxidation resistance of alloy at 1000°C.

1. Introduction

NiCrCoAlY alloys are often used as bond coatings of thermal barrier coatings (TBCs) to protect the substrate from oxidation at high temperature and to provide the necessary adhesion of the ceramic to the substrate [1-3]. Some authors [4-7] indicated that the protection offered by MCrAlY (M=Ni, Co or a combination) alloys against high temperature oxidation relies on the ability of the alloy to develop and maintain a continuous, dense and slow growing α-Al_2O_3 scale. The formation of a continuous of alumina (Al_2O_3) layer during the oxidation of the substrate at high temperatures could result in a dramatic slowing down of the oxidation process, because Al_2O_3 formation has a slower rate of oxidation compared to other oxidations. Generally, the protectiveness of the alloy surface at long-term stage is frequently determined by the initial stage of oxidation [8-10].

Besides alumina, chromia (Cr_2O_3) also plays an important role during the high temperature oxidation [11-13]. However, the effect of the interaction among the oxides on the oxidation resistance of alloy has not been discussed in detail. In particular, there has been a lack of attention to the initial stages of oxidation on NiCoCrAlY alloy to date.

Raman spectroscopy has been used as a non-destructive technique for determining the stresses in oxide scales for decades due to the bands in the Raman spectra of specimens shift with pressure [11-13]. The salient features of the Raman technique are that it does not require a special environment, and it provides a high resolution.

The aim of this study is to improve the service life of the alloys. The evolution of the oxide scale on the surface of NiCoCrAlY alloy at initial stage oxidized at 800°C-1000°C were investigated. After reporting the experimental results, a method to improve the oxidation resistance was proposed by utilizing the interaction cha-

racteristics of Al_2O_3 and Cr_2O_3 growth.

2. Experimental

The original powder was commercially available, and its component was 6.5%Co, 17.8%Cr, 3.7%Al, 0.5%Y, balance Ni (wt.%) with an average particle size of 16.34 μm.

The powder was heated and compacted into the form of a cylindrical rod of green density equal to 89 ± 5% of its theoretical density at inner temperature of 800°C for 2 hours with a pressure of 300 MPa. Subsequently, the rod was annealed in vacuum at 1000°C for 1 hour in order to homogenize and recrystallize the alloy.

Disc shaped specimens (diameter 15 mm and thickness 1 mm) were cut from the rod using spark-machining. The specimen surface was ground and polished. After each preparation step the specimens were thoroughly cleaned ultrasonically with alcohol.

Isothermal oxidation was performed in static air at 1 atm pressure in a resistance furnace which has a maximum operating temperature of 1300°C. All the specimens were put into the furnace at the same time after the test temperature was reached. Then, oxidized specimens were removed out from the furnace after a chosen time and air-cooled to room temperature. The initial oxidation tests were performed at 800°C, 900°C and 1000°C for 2, 4, 8 and 16 hours.

A thermal cycling oxidation test was conducted at 1000°C for 200 hours. In order to keep consistent of oxidation condition in the test, the specimens were pre-oxidized at 900°C and 1000°C for 16 hours. Then the oxidation behavior of the specimens was evaluated by measuring the weight gains of the samples for 184 hours. The 12-hour cycle consisted of 11 hours holding at 1000°C, followed by cooling in air for 1 hour. The precision of the balance was 0.1 mg.

Raman spectroscopy was used here in order to determine the stresses in chromia scales formed at 900°C and 1000°C on NiCoCrAlY alloy. Chromia has the same structure as corundum, and therefore it should have seven Raman active bands (A_{1g} + $5E_g$) [11-13]. The most intense mode is the 549 cm^{-1} A_{1g} vibration [11] and this one was used for monitoring the stress.

The spectroscopy was measured at room temperature using the Renishaw Ramanscope 1000 (Renishaw™, Gloucestershire, UK) in conjunction with an Olympus BH-2 microscope. During the measurements, the laser (He–Ne, 632.8 nm) was focused at a position on the surface of the sample and the laser spot size was set about 3–5 μm. The Raman spectroscopy acquired was analyzed by the commercial Renishaw WiRe software to obtain the peak shift fitted by Gaussian–Lorentzian function.

The surface morphologies and polished cross sections of the specimens were observed using a scanning elec-

tron microscopy (SEM) (JSM-7000F). The chemical composition of the oxides was determined qualitatively by energy-dispersive X-ray analysis (EDX). The phases in the oxide scales were analyzed using an X-ray diffraction (XRD) (Rigaku D, CuKα radiation).

3. Results and Discussion

3.1. The Oxides on the Surface after Initial Oxidation

X-ray diffraction patterns of NiCoCrAlY alloy after oxidation for 16 hours at 800°C, 900°C and 1000°C are shown in **Figure 1**. Results from the study show that the oxides on the surface of alloy which was heated to 800°C for 16 hours are composed of Cr_2O_3, a few θ-Al_2O_3 and $YAlO_3$, trace α-Al_2O_3 and NiO. It was found that however, oxides θ-Al_2O_3 and $YAlO_3$ did not form at 900°C and 1000°C. The spinel oxide, $NiCr_2O_4$, began to exist after 16 hours of oxidation at 900°C.

According to the intensity of diffraction peaks, the relative oxidation rates of Cr_2O_3 and α-Al_2O_3 phases on the surface of alloy oxidized from 2 hours to 16 hours at 800°C, 900°C and 1000°C are shown in **Figure 2**.

From **Figure 2(a)**, **Figure 2(b)**, it can be seen that the relative quantities of Al_2O_3 and Cr_2O_3 increased quickly in the first two hours. After that, the oxidation rate of Al_2O_3 rises slowly while the relative quantities of Cr_2O_3 at 900°C and 1000°C keep fluctuating. The increase of quantities of α-Al_2O_3 resulted from dense α-Al_2O_3 oxide forming and θ-Al_2O_3 transforming. The fluctuation of quantities of Cr_2O_3 at 900°C and 1000°C may have been caused by spinel oxides $NiCr_2O_4$ formation which consumed Cr_2O_3. With the increased temperature or prolonged exposure time, NiO eventually became destabilized and reacted with Cr_2O_3 to form a thin spinel layer of $NiCr_2O_4$, which was thermodynamically more stable [9,14-16]. The competition between the consumption of
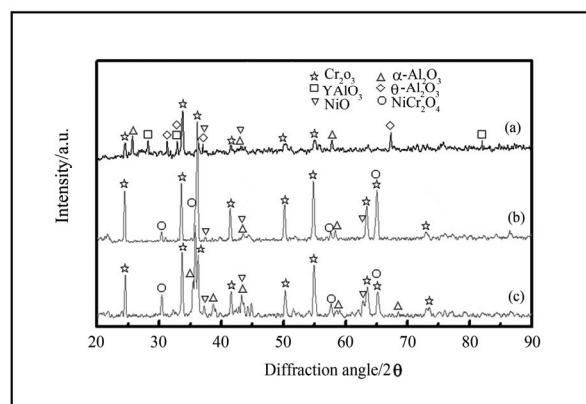

Figure 1. X-ray diffraction patterns of Ni6.5Co17.8Cr3.7 Al0.5Y alloy (oxidized for 16 h) at (a) 800°C; (b) 900°C and (c) 1000°C.
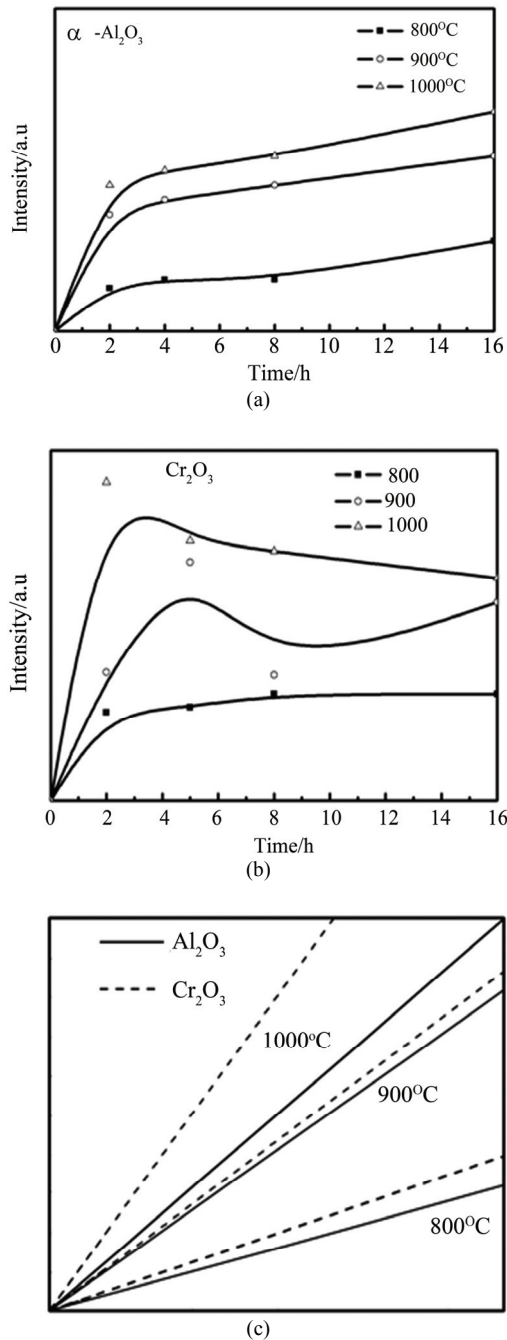
(a)

(b)

(c)

Figure 2. Relative quantities of Cr$_2$O$_3$ and α-Al$_2$O$_3$ phases on the surface of alloy vs. time: (a) α-Al$_2$O$_3$; (b) Cr$_2$O$_3$; (c) the relative oxidation rates of Cr$_2$O$_3$ and α-Al$_2$O$_3$ at the second hour at 800°C, 900°C and 1000°C.

Cr$_2$O$_3$ and the formation of Cr$_2$O$_3$ determined the outline of curve.

Figure 2(c) shows that the relative oxidation rates of α-Al$_2$O$_3$ and Cr$_2$O$_3$ increased with temperature in the second hour from 800°C to 1000°C. Also, it can be observed that the growth rate of α-Al$_2$O$_3$ is similar to that of Cr$_2$O$_3$ at 900°C. However, at 1000°C, the increase of

growth rate of α-Al$_2$O$_3$ is not as much as the growth rate of Cr$_2$O$_3$.

3.2. The Cracking and Closure of the Oxide Scale in Initial Oxidation

A SEM image of the specimen surface oxidized in air for up to 16 hours at 800°C is shown in **Figure 3(a)**. **Figure 3(b)** is at a higher magnification. These images show that some protrudes, pores and pits are presented on the surface, but few cracks appeared.

The whisker or needlelike oxide phase is observed. The EDX analysis (**Figure 3(c)**, **Figure 3(d)**) of the oxide whiskers produced Al, Cr and O peaks, which is qualitatively identified as Al$_2$O$_3$ and Cr$_2$O$_3$ phases. As the θ-Al$_2$O$_3$ phase usually grows in a needlelike, whiskerlike or bladelike morphology and α-Al$_2$O$_3$ grows in a weblike or dense equiaxed structure [14,17], these bladelike oxides should be θ-Al$_2$O$_3$.

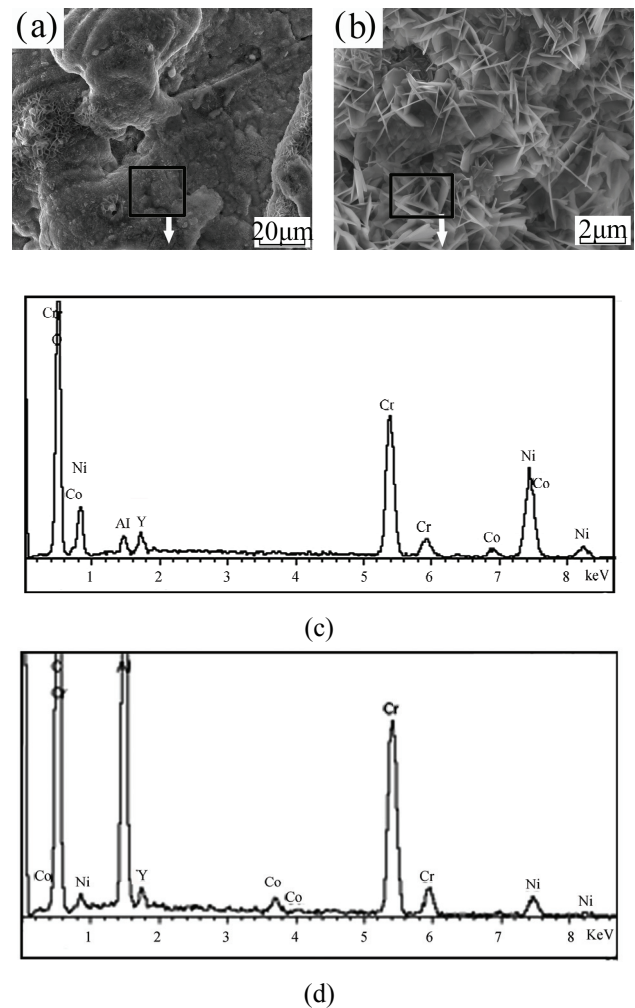(a)   (b)

(c)

(d)

Figure 3. SEM images of the specimen surface (oxidized for 16h at 800°C) (a) surface image; (b) higher magnification; (c) and (d) EDX analysis in selected region.

The surface images of specimens exposed at 900°C and 1000°C in a static atmosphere for 16 hours are shown in **Figure 4(a)**, **Figure 4(b)**. It was found that specimens covered with fine oxide particles. It was also observed irregular ditches on the surface at both temperatures and cracks in the oxide scale. The cracks became more serious as the temperature increased. The spallation on the surface of the oxidized specimen was unavoidable.

It may have resulted from the stress during the cooling and heating process and the mismatch between the expansion coefficients of oxides and alloys.
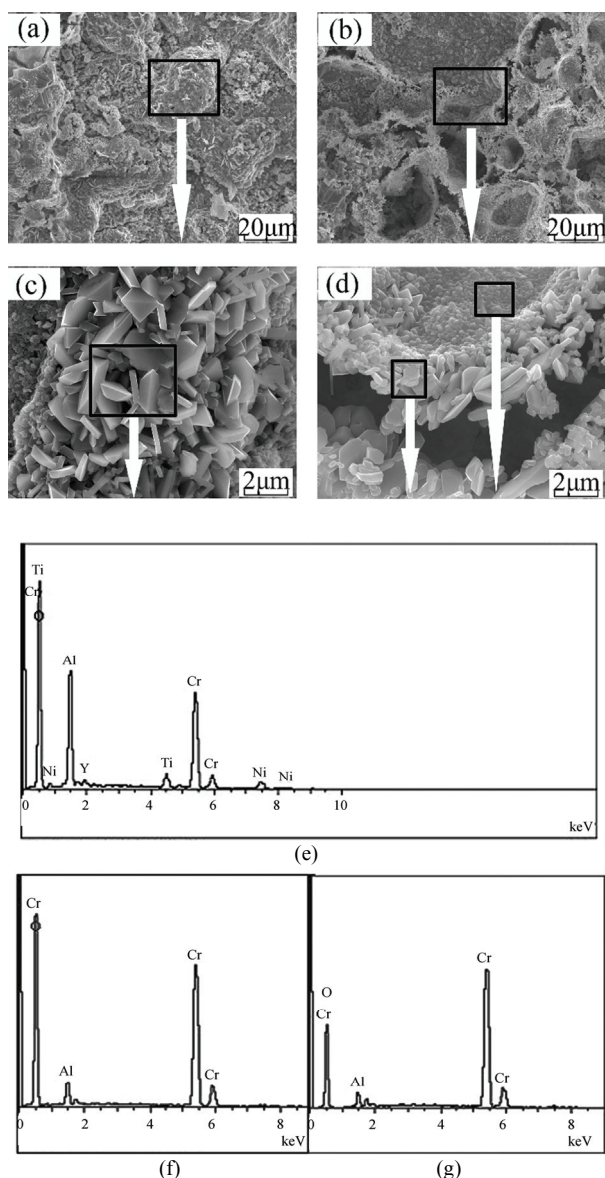

Figure 4. The surface images of specimens (oxidized for 16h at 900°C and 1000°C) (a) specimens oxidized at 900 °C; (b) specimens oxidized at 1000°C; (c) higher magnification of Figure. 4(a); (d) higher magnification of Figure. 4(b); (e), (f) and (g) EDX analysis in selected regions.

EDX analysis (**Figure 4(f), 4(g)**) shows that the oxides around the cracks are Cr_2O_3 (**Figure 4(d)**). This indicates that these cracks were caused by the Cr_2O_3 oxide scale broke during the oxidation. At the same time, it was observed that some oxides were growing from the cracks in **Figure 4(c)**. By EDX analysis, it is confirmed that these oxides are α-Al_2O_3 and Cr_2O_3. It can be speculated that, at 900°C, α-Al_2O_3 grew form the bottom of the Cr_2O_3 oxide scale cracks, which filled in the cracks and made the oxide scale dense. Contrasting **Figure 4(a)** with **Figure 4(b)**, it is can be seen that the cracks in the oxide scale at 1000°C are more than those at 900°C. There are more irregular ditches observed among the Cr_2O_3 oxide scale but not so much α-Al_2O_3 fill in the cracks.

Form **Figure 2**, we observe that the growth rate of α-Al_2O_3 is similar to that of Cr_2O_3 at 900°C. Though the spallation on the Cr_2O_3 scale was unavoidable, α-Al_2O_3 could preferably nucleate during oxidation on the surface in some cracks of the oxide scale at 900°C where they could grow and fill in those ditches. With the density of the oxide scale increased, both the oxygen and cation diffusion rate decreased. Thus the ability of oxidation resistance would be improved. However, the growth rate of Cr_2O_3 is much larger than that of α-Al_2O_3 at 1000°C. When the oxides on the surface of the alloy grew at a larger rate, the oxide scale cracked and spalled easily. Because of the cracks, oxygen diffused through the oxide scale easily to contact the oxide–alloy interface, which speeded up the oxidation of alloy greatly.

The cross-sectional microstructure and the elemental maps of the NiCoCrAlY specimens obtained by SEM and EDX after oxidation at three different temperatures for 16 hours are shown in **Figure 5**. The elemental concentration regions of O, Cr and Al are presented in the **Figures 5(a_2)-5(c_4)**.

From **Figure 5(a_2)**, **Figure 5(b_2)** and **Figure 5(c_2)**, it was found that the thickness of the oxide layer increases with the temperature rising. A continual oxide layer formed at 900°C, and it became thicker at 1000°C. The Cr_2O_3 phase dominated in the oxide layers (**Figure 5(a_3)**, **Figure 5(b_3)** and **Figure 5(c_3)**) while the Al_2O_3 phase was not abundant in these environments (**Figure 5(a_4)**,
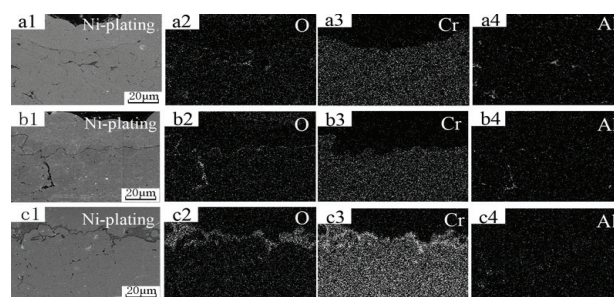

Figure 5. The cross-sectional microstructure and the elemental maps of NiCoCrAlY alloy (oxidized for 16 h) at (a) 800°C; (b) 900°C and (c) 1000°C.

ENG

Figure 5(b₄) and **Figure 5(c₄)**). This indicated that Cr_2O_3 formed at the initial oxidation stage. Some brightness Al-containing regions denote the Al_2O_3 which filled in the Cr_2O_3 ditches (**Figure 5(b₄)**). This is in good agreement with the XRD and surface microstructure results.

Though a continuous layer of Al_2O_3 was not appeared at the onset of the oxidation, an inner zone of isolated Al-containing phase could be observed at all three temperatures in **Figure 5(a₄)**, **Figure 5(b₄)** and **Figure 5(c₄)**. This was in good agreement with the literature [10] and the Al-containing phase should be α-Al_2O_3. The lateral growth of α-Al_2O_3 precipitates occurred until they coalesce into a continuous α-Al_2O_3 layer.

3.3. Stress Determination

Figure 6 shows the Raman spectrum obtained from the oxide scale formed on the surface of NiCoCrAlY alloys oxidized at 900°C and 1000°C for 16h. The only band which is well-defined in both spectra is the A_{1g} mode at 549 cm^{-1} in Mougin *et al.*'s work [11]. In the scales, this mode shifts to 549.53 cm^{-1} for 900°C specimen and 554.34 cm^{-1} for 1000°C specimen respectively, resulting in the observed shifts are equal to 0.53 cm^{-1} and 5.34 cm^{-1} respectively. Using the law given by Mougin et al. [11] for the frequency dependence with pressure, *i.e.*, 0.307 ± 0.005 GPa/cm^{-1}, it gives the stress values of 0.163 ± 0.005 GPa for 900°C specimen and 1.639 ± 0.005 GPa for 1000°C specimen respectively. The shift direction corresponds to compressive stress.

The results exhibited here agree with the previous discussion. The higher growth rate of Cr_2O_3 at 1000°C resulted in a higher stress than the stress generated at a lower temperature. The structure under high stress condition was easier to crack, spall and fracture and was more difficult to self-healing by the Al_2O_3 growth simultaneously.
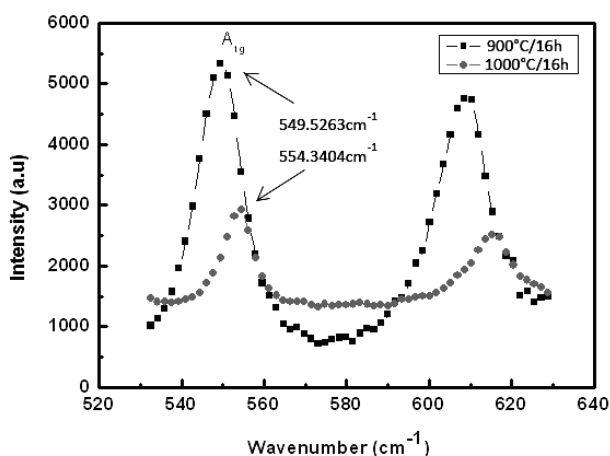

Figure 6. Raman spectrum for the chromia formed on Ni-CoCrAlY alloys oxidized for 16 h at 900°C and 1000°C.

3.4. The Effect of the Preoxidation Treatment on the Oxidation Resistance

Due to the different growth characteristics of α-Al_2O_3 and Cr_2O_3 at different temperatures at initial stage of oxidation, two groups of specimen were conducted. One was directly oxidized at 1000°C for 200 hours. The other one was subjected to a preoxidation treatment at 900°C for 16 hours first, aiming to repair micro-cracks in the Cr_2O_3 scale by subsequent growth of α-Al_2O_3, then oxidized at 1000°C for 184 hours. The oxidation behavior of the specimens was evaluated by a cyclic oxidation test.

Figure 7 represents the weight gain as a function of time for the cycle oxidation at 1000°C. In the figure, curve (a) indicates the specimen directly oxidized at 1000°C for 200 hours and curve (b) indicates the specimen which preoxidixed at 900°C. At the onset of the oxidation, the rate of weight gain of the specimen preoxidized at 900°C was slower than that of 1000°C. After the sharp increase of weight gain at the initial oxidation stage, both of the kinetic curves showed an extensive period of very slow weight gain. Obviously, the alloy which preoxidised at 900°C showed lower weight gains than that of 1000°C.

With oxidation depth increased, oxygen activity reduced unceasingly, Al_2O_3 precipitates would nuclear in subsurface of the alloy but no longer for Cr_2O_3. This could explain that why the relative quantity of α-Al_2O_3 at 900°C was larger than that at 1000°C. At 1000°C, a great amount of Cr_2O_3 formed by the contact between Cr irons and the oxygen through the severe cracks.

4. Conclusions

Initial oxidation tests of Ni-6.5Co-17.8Cr-3.7Al-0.5Y alloy specimens was performed at 800°C, 900°C and 1000°C for 16 hours. Cr_2O_3 was the predominant phase at all three temperatures and the dense Cr_2O_3 scale play-
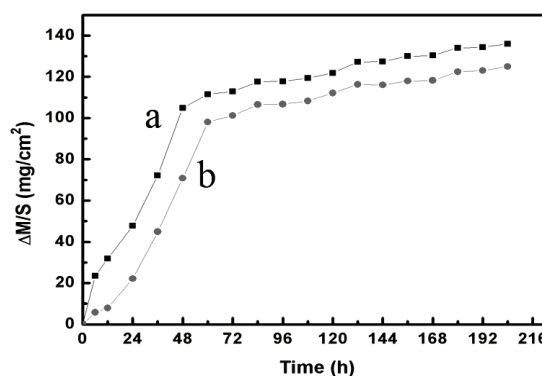

Figure 7. Weight gain of specimens vs. time in the cyclic oxidation at 1000°C for 200 h (a) directly oxidized at 1000°C; (b) preoxidation treatment at 900°C for 16 h.

ed an important role in protecting against cracking and oxidation in the first 16 hours of the isothermal oxidation at 800°C. $YAlO_3$ phase was only observed at 800°C. That the growth rate of α-Al_2O_3 was similar to that of Cr_2O_3 at 900°C lead to the α-Al_2O_3 could grow and fill in the ditches on the Cr_2O_3 scale. However, the growth rate of Cr_2O_3 at 1000°C was much larger and produced higher stress than that at 900°C, so that the α-Al_2O_3 grown from the Cr_2O_3 oxide ditches was not enough to fill in these cracks. Though the spallation on the surface of oxidized specimen was unavoidable at the higher temperature (900°C and 1000°C), a preoxidation treatment at 900°C for 16 hours can cause α-Al_2O_3-dispersions-in-Cr_2O_3 scale formed on the surface of the specimen. This could improve the oxidation resistance of NiCoCrAlY alloy in the thermal cycling oxidation.

5. Acknowledgment

6. References

[1] N. P. Padture, M. Gell and E. H. Jordan, "Thermal Barrier Coatings for Gas-Turbine Engine Applications," *Science*, Vol. 296, No. 5566, 2002, pp. 280-284.

[2] A. G. Evans, D. R. Mumm, J. W. Hutchinson, G. H. Meier and F. S. Pettit, "Mechanisms Controlling the Durability of Thermal Barrier Coatings," *Progress in Materials Science*, Vol. 46, No. 5, 2001, pp. 505-553.

[3] Y. Fengling and T. D. Bennett, "Phase of Thermal Emission Spectroscopy for Properties Measurements of Delaminating Thermal Barrier Coatings," *Journal of Applied Physics*, Vol. 98, No. 10, 2005, pp. 103501-103508.

[4] R. Panat, S. L. Zhang and K. J. Hsia, "Bond Coat Surface Rumpling in Thermal Barrier Coatings," *Acta Materialia*, Vol. 51, No. 1, 2003, pp. 239-249.

[5] B. Wang, J. Gong, A. Y. Wang, C. Sun, R. F. Huang and L. S. Wen, "Oxidation Behaviour of Nicraly Coatings on Ni-Based Superalloy," *Surface & Coatings Technology*, Vol. 149, No. 1, 2002, pp. 70-75.

[6] U. Schulz, C. Leyens, K. Fritscher, M. Peters, B. Saruhan-Brings, O. Lavigne, J. M. Dorvaux, M. Poulain, R. Mevrel and M. L. Caliez, "Some Recent Trends in Research and Technology of Advanced Thermal Barrier Coatings," *Aerospace Science and Technology*, Vol. 7, No. 1, 2003, pp. 73-80..

[7] R. A. Mahesh, R. Jayaganthan and S. Prakash, "Microstructural Characteristics and Mechanical Properties of HVOF Sprayed Nicral Coating on Superalloys," *Journal of Alloys and Compounds*, Vol. 468, No. 1-2, 2009, pp. 392-405.

[8] T. F. An, H. R. Guan, X. F. Sun and Z. Q. Hu "Effect of the Theta-Alpha-Al_2O_3 Transformation in Scales on the Oxidation Behavior of a Nickel-Base Superalloy with an Aluminide Diffusion Coating," *Oxidation of Metals*, Vol. 54, No. 3-4, 2000, pp. 301-316.

[9] S. O. Moussa and K. Morsi, "High-Temperature Oxidation of Reactively Processed Nickel Aluminide Intermetallics," *Journal of Alloys and Compounds*, Vol. 426, No. 1-2, 2006, pp. 136-143.

[10] T. J. Nijdam, N. M. van der Pers and W. G. Sloof, "Oxide Phase Development upon High Temperature Oxidation of Gamma-Nicral Alloys," *Materials and Corrosion-Werkstoffe Und Korrosion*, Vol. 57, No. 3, 2006, pp. 269-275.

[11] M. Kemdehoundja, J. F. Dinhut, J. L. Grosseau-Poussard and M. Jeannin, "High Temperature Oxidation of $Ni_{70}Cr_{30}$ Alloy: Determination of Oxidation Kinetics and Stress Evolution in Chromia Layers," *Materials Science and Engineering A*, Vol. 435-436, No. 5, 2006, pp. 666-671.

[12] G. Calvarin, A. M. Huntz, A. Hugot Le Goff, S. Joiret and M. C. Bernard, "Oxide Scale Stress Determination by Raman Spectroscopy Application to the $Nicr/Cr_2O_3$ System and Influence of Yttrium," *Scripta Materialia*, Vol. 38, No. 11, 1998, pp. 1649-1658.

[13] P. Kofstadt, "*High Temperature Corrosion*," Elsevier, New York, 1988.

[14] D. Lee, M. L. Santella, I. M. Anderson and G. M. Pharr "Thermal Aging Effects on the Microstructure and Short-Term Oxidation Behavior of a Cast Ni_3Al Alloy," *Intermetallics*, Vol. 13, No. 2, 2005, pp. 187-196.

[15] S. Seal, S. C. Kuiry and L. A. Bracho, "Surface Chemistry of Oxide Scale on IN-738LC Superalloy: Effect of Long-Term Exposure in Air at 1173 K," *Oxidation of Metals*, Vol. 57, No. 3-4, 2002, pp. 297-322.

[16] S. C. Choi, H. J. Cho and D. B. Lee, "Effect of Cr, Co, and Ti Additions on the High-Temperature Oxidation Behavior of Ni_3Al," *Oxidation of Metals*, Vol. 46, No. 1-2, 1996, pp. 109-127.

[17] H. H. Angermann, K. Nishi, Y. Aono, M. Inagaki and H. Kodama, "Evolution of Oxides on Ni-Base ODS Superalloys," *Oxidation of Metals*, Vol. 48, No. 1-2, 1997, pp. 1-39.